Desalination 464 (2019) 76–83

Contents lists available at ScienceDirect

Desalination

journal homepage: www.elsevier.com/locate/desal

Scaling prevention of thin film composite polyamide Reverse Osmosis membranes by Zn ions

Mujahid Aziz*, Godwill Kasongo

Department of Chemical Engineering, Cape Peninsula University of Technology, P.O. Box 652, Cape Town 8000, South Africa

GRAPHICAL ABSTRACT

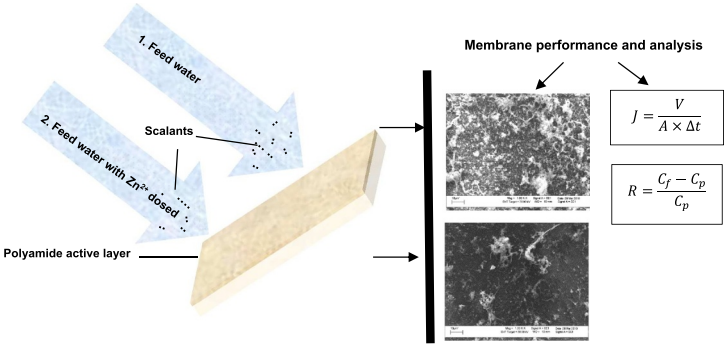

ARTICLE INFO

Keywords:
Brackish water
Membrane
Fouling
Scaling
Reverse Osmosis (RO)
Anti-scalant
Zinc (Zn)
Flux

ABSTRACT

On the West Coast of South Africa, there is an abundance of brackish groundwater. Reverse Osmosis membrane systems are used to make the borehole water fresh. Unfortunately, the salts that are removed from the water, precipitates on the membrane surface, thus, decreasing the overall process efficiency. In this study, the use of Zn^{2+} ions as an anti-scalant was investigated in terms of feasibility in the treatment of brackish water influent. Experimental tests were conducted on a bench scale unit, followed with a pilot plant thereafter. Three commercial membranes were exposed to natural groundwater scaling. The first, commercial anti-scalant treatment, second, anti-scalant treatment with Zn^{2+} ions and the third, untreated. The results, after a period of close to 5 months, showed that the flux of the membranes treated with commercial (32.78 $L{\cdot}m^{-2}{\cdot}h^{-1}$) and zinc (30.80 $L{\cdot}m^{-2}{\cdot}h^{-1}$) ions anti-scalant was higher than the untreated membrane flux (25.56 $L{\cdot}m^{-2}{\cdot}h^{-1}$), which decreased continuously.

1. Introduction

Reverse Osmosis (RO) has emerged as one of the promising large-scale processes for the economical removal of salts from seawater and brackish water, due to high volumes of fresh water needed in many parts of the world for agricultural, industrial and domestic use [1–3].

However, several studies have reported inorganic fouling of RO membranes, called scaling, as a major concern in water purification processes [4–7]. Scaling occurs when minerals constituents of the feed water precipitate on the surface of the membrane [6,8,9] after they have reached a state of saturation [10,11]. Both mechanisms, participate in the scaling process [3]. Various studies have shown that ionic constituents in feed water in desalination processes may combine under suitable conditions to form salts as $CaCO_3$, $CaSO_4$, $Mg(OH)_2$, $BaSO_4$,

* Corresponding author.
E-mail address: azizm@cput.ac.za (M. Aziz).

https://doi.org/10.1016/j.desal.2019.04.021
Received 3 December 2018; Received in revised form 8 April 2019; Accepted 18 April 2019
Available online 28 April 2019
0011-9164/

$CaSO_4{\cdot}2H_2O$, $SiSO_4$, SiO_2 and more which are known as slightly soluble and scales forming salts [3,4,6,11]. Simulated brackish water has a silt density index (SDI) range between 1.0 and 1.6, indicating membrane scaling potential [7,12]. It is known that scale formation impairs the performance of RO processes as it affects the salt rejection, the permeate flux as well as the membrane lifespan [3,10]. The scale formation mechanism generally takes place in two crystallization pathways: heterogeneous and homogeneous. Heterogeneous crystallization is when precipitation takes place at the surface of the membrane, and homogeneous crystallization is when precipitation takes place in the bulk solution [3]. The acidification of feed water; use of anti-scalants (AS); chemicals; control of RO system operating conditions; as well as the softening of feed water, are the techniques used, to prevent scaling [6]. Precipitation on the membrane surface can be prevented by using effective anti-scalant [11,13]. These anti-scalants consist of a single component or a mixture of components which has the molecular weight in the ranges between 1000 and 3500 g/mol [14]. It disrupts the formation of precipitates in one of three ways, namely: threshold inhibition; crystal modification and dispersion [13]. The use of anti-scalant for targeted water conditions can assist with RO system performance and reduce cost by minimizing frequent membrane cleaning and replacement [14].

Metallic ion impurities, notably Zn^{2+}, can hinder $CaCO_3$ precipitation from hard water and alter the crystal morphology [12,13,15,16]. Zn^{2+} causes a substantial increase in induction time and causes the formation of $CaCO_3$ in the aragonite form rather than the calcite form. Therefore, Zn^{2+} can potentially be used as anti-scalant for brackish feed water [15], where $CaCO_3$ is the main potential scalant. The main advantages of using Zn^{2+} are that it can be conveniently dosed (e.g. as Cu—Zn alloy); is environmentally friendly; much lower running cost; the availability of Zn^{2+} metal; cheap Zn^{2+} generation and minimal waste disposal. Furthermore, the product water meets the drinking water criteria with an upper limit of 5 ppm [12]. In this study, the aim was to assess the use of anodic Zn as an anti-scalant and compare it with a commercially available anti-scalant chemical, in the scaling of RO membranes when treating brackish water.

2. Materials and methods

2.1. Laboratory tests on the scaling inhibition

2.1.1. Chemicals

Analytical grade calcium chloride ($CaCl_2$), magnesium sulfate ($MgSO_4$) and Sodium hydrogen carbonate ($NaHCO_3$) were obtained from Merck. Anti-scalant phosphonic acid ($H_2O_3P^+$) (Vitec 3000) was obtained from Avista Technologies. In the preparation of synthetic brackish water, the mass of various compounds are presented in Table 1 where it was used per 100 L of solution ([9,12,15]). All solutions were prepared with purified MilliQ water.

Table 1
The composition of the synthetic brackish water [9].

Description/(unit)	Concentration
$CaCl_2$ (g/L)	0.61
$MgSO_4$ (g/L)	0.05
$NaHCO_3$ (g/L)	0.51
TDS (g/L)	1.140
pH (–)	7.96
Temp. (°C)	22–24
LSI (–)	0.750
SDI range [7,12]	1.0–1.6

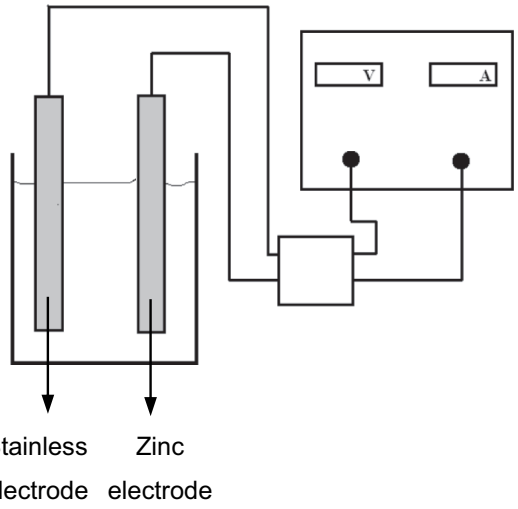

Fig. 1. Zn^{2+} ions generation through the electrochemical cell [15].

2.2. Experimental procedure

2.2.1. Zn^{2+} ions generation using a bench scale electrochemical cell

Zn^{2+} ions were generated through the electrolytic cell with filtered water. The cell had two nodes; the first connected to the ampere meter and the second connected to the stainless steel metal immersed into the beaker to complete the circuit. The outlet node of the ampere meter was connected to the zinc metal immersed into the beaker as shown in Fig. 1. Zinc metal was used as a source of zinc ion. A multi-parameter ion specific meter was used to measure the Zn^{2+} ions in the solution.

2.2.2. On-line Zn^{2+} ion generation on Lab scale RO system

Experiments were conducted in a continuous flow SEPA CF II membrane element cell (Fig. 2). Experiments were conducted at flux ranges between 26 and 30 $L{\cdot}m^{-2}{\cdot}h^{-1}$, ambient temperature and applied pressure of 10 bar. The membrane used was a high rejection thin film composite (TFC) polyamide spiral wound RO membrane (Filmtec XLE 4040) cut into flat sheets. Membrane characteristics are shown in Table 2 below.

The experimental system was operated as shown in Fig. 2. The laboratory tests consisted of three parts; the first of which the membrane performance was tested with raw synthetic brackish water, followed by raw synthetic brackish water spiked with a chemical anti-scalant and lastly, when the membrane performance was tested with raw synthetic brackish water in which Zn^{2+} ions was dosed constantly. The Zn^{2+} ions were generated by using an electrolytic cell. The inhibition effectiveness of Zn^{2+} ions was assessed by comparing membrane flux decline J ($L{\cdot}m^{-2}{\cdot}h^{-1}$), at various experimental run conditions. The salt rejection R (%) was monitored to evaluate membrane stability. The permeate flux and salt rejections were calculated using Eqs. (1) and (2) respectively:

$$J = \frac{V}{A \times \Delta T} \tag{1}$$

$$R = \frac{C_f - C_p}{C_f} \times 100 \tag{2}$$

where V, A and ΔT are the volume of permeate (L), the effective area of the membrane (m^2) and the interval time (h) respectively. In Eq. (2), C_f (μS/cm), and C_p (μS/cm) are the feed conductivity and permeate conductivity respectively.

2.3. RO pilot plant

The pilot plant consisted of three TFC polyamide RO membrane

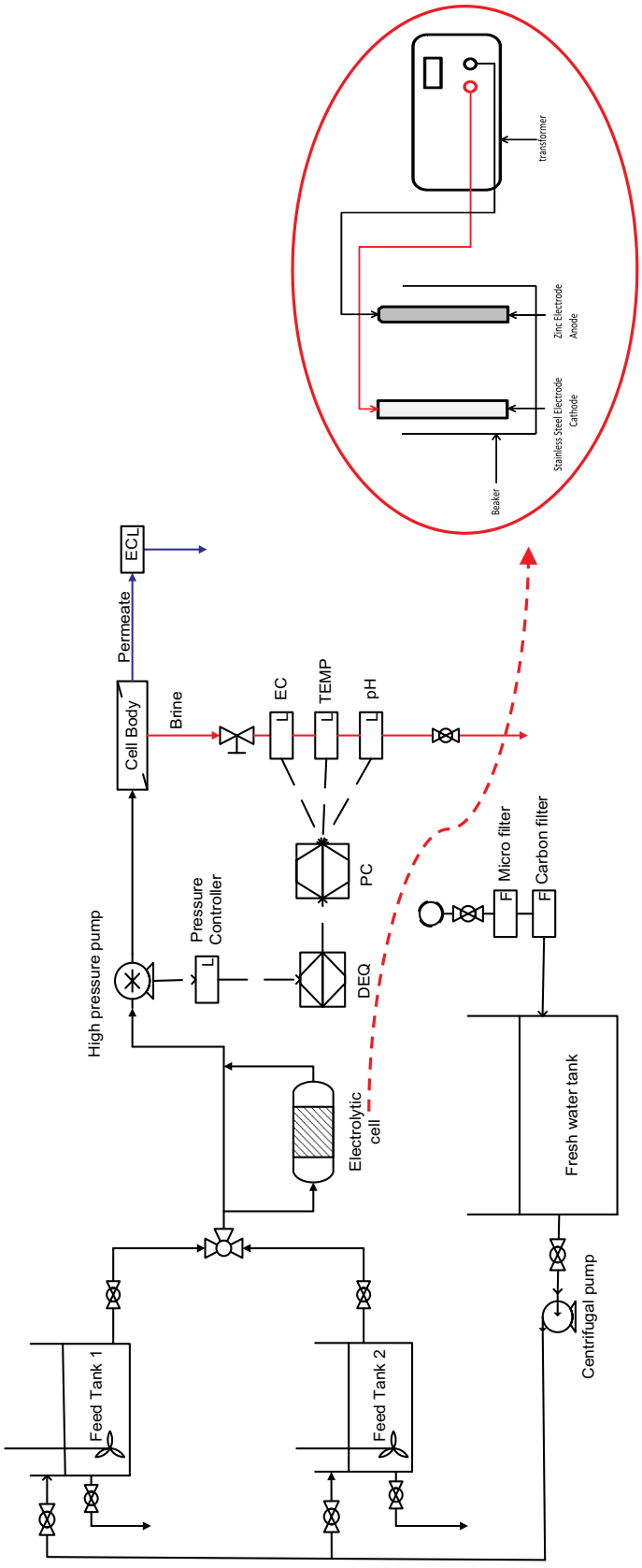

Fig. 2. RO membrane system with online zinc generation [15].

Table 2
TFC RO membrane characteristics (Dupont.com, 2017).

Parameter (unit)	
Feed water concentration, TDS (mg/L)	2600
Feed water pressure (bar)	6.9
Recovery rate (%)	15
Water pH (–)	2–11
Salt rejection (%)	99.0
Product flow rate (m^3/day)	0.750

modules (Filmtec XLE 4040), in parallel, which was subjected to different running conditions. The first membrane was subjected to only raw feed with no anti-scalant chemical supplements; the second was treated with feed dosed with commercial anti-scaling chemical and the third was treated with Zn^{2+} ions. The Zn^{2+} ions were generated by use of an electrolytic cell. Raw brackish water that underwent a primary treatment sedimentary process was used as the feed to the pilot plant (Fig. 3). The permeate conductivity and flow rates of the above-mentioned membranes were recorded.

2.4. Analytical method — cell

Foulants deposited on the membrane surface after scaling experimental runs were characterized by Leo 1430VP scanning electron microscopy (SEM). Membrane samples were cut and sputter-coated with gold prior to capturing of SEM images. Optical microscopy (OM) was additionally conducted to confirm that scaling has occurred on the surface of the membrane.

3. Results

3.1. Effects of electrochemical cell current on Zn^{2+} generation

Preliminary experiments were conducted to assess the effects of voltage and current density on the generation of Zn^{2+} ions. From the results obtained in Fig. 4 (Left), when the voltmeter is set at 2 V it can be seen that the zinc ions generation increases as the current density decreases with time. This could be explained by the fact that, at high current, zinc ions tend to deposit on the stainless steel electrode and that generates impurities which are detrimental to zinc ion generation [15]. The generation of zinc ions was not constant with time because of the fluctuation of the current during the operation.

It is further noticed that zinc ions generation decreased with an increase in voltage, and no Zn^{2+} ions were generated at 6 V as shown in Fig. 4 (Right). This could be due to oxidation reaction occurring that caused the deposition of zinc on the stainless steel electrode hence, impeding the electrolytic process of zinc generation [15].

3.2. Effect of anti-scalant on RO membrane performance

3.2.1. Effect of Zn^{2+} ions generation voltage on membrane performance

Effects of Zn^{2+} ions generation voltage was further related to membrane performance. Fig. 5 below shows averages of permeate flux and salt rejections after 120 min of experimental runs. Different flux values were obtained for the three voltages applied. It can be seen that the permeate flux decreases with an increase in voltage. The highest permeate flux of 29 $L{\cdot}m^{-2}{\cdot}h^{-1}$ was obtained at the lowest voltage of 2 V and at a Zn^{2+} ions concentration of 0.2 ppm. The result shows that change in Zn^{2+} ions voltage generation did not affect the membrane salt rejection.

3.2.2. Comparison between Zn^{2+} ions and $ZnSO_4$ effects on membrane performance

Two different procedures for a Zn^{2+} ion generation were tested. Firstly, zinc ions were generated by dosing $ZnSO_4$ into the feed tank. Secondly, Zn^{2+} ions were generated online using a voltaic cell in the system. Zn ions were automatically generated as the salt dissolved in water. Fig. 6 shows the effects of these two procedures on the performance of the membrane with time.

It can be observed during the $ZnSO_4$ experimental run in Fig. 6 (left), that the flux increased with an increase of $ZnSO_4$ concentration.

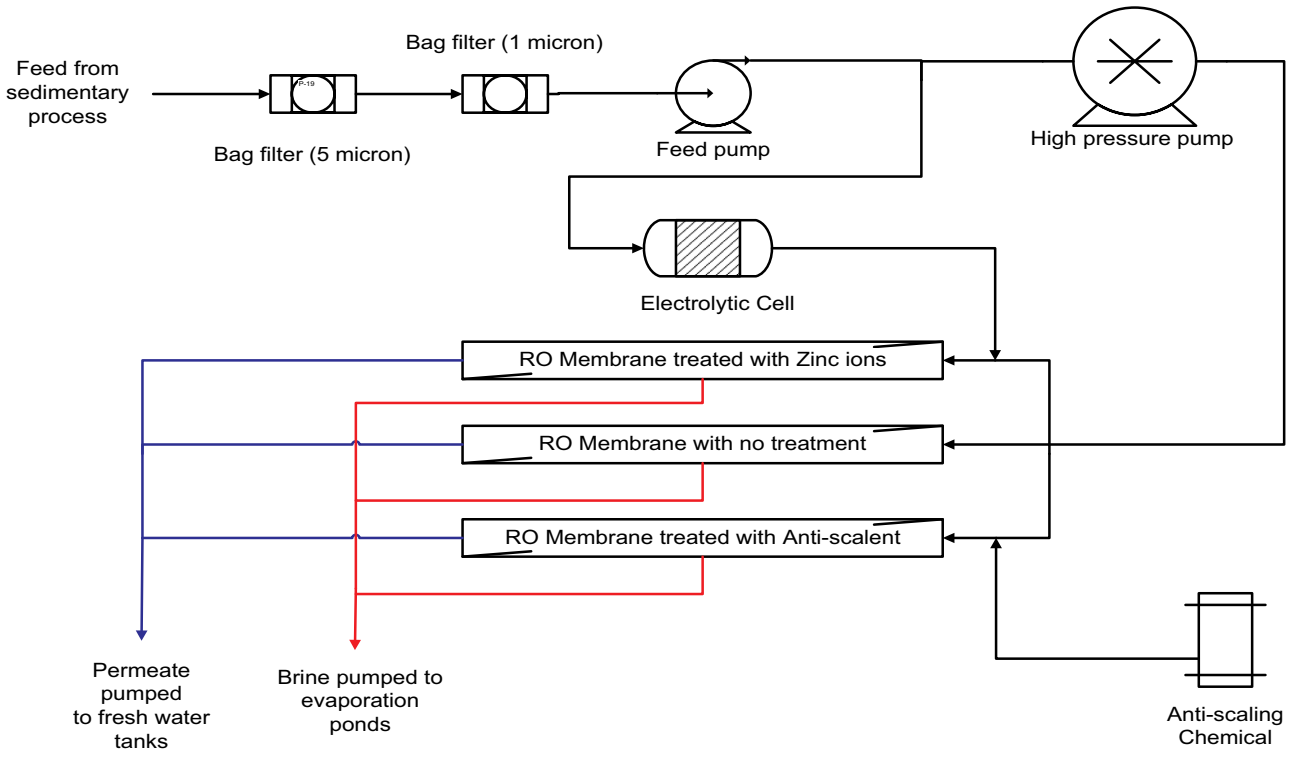

Fig. 3. Process flow diagram of a pilot plant [15].

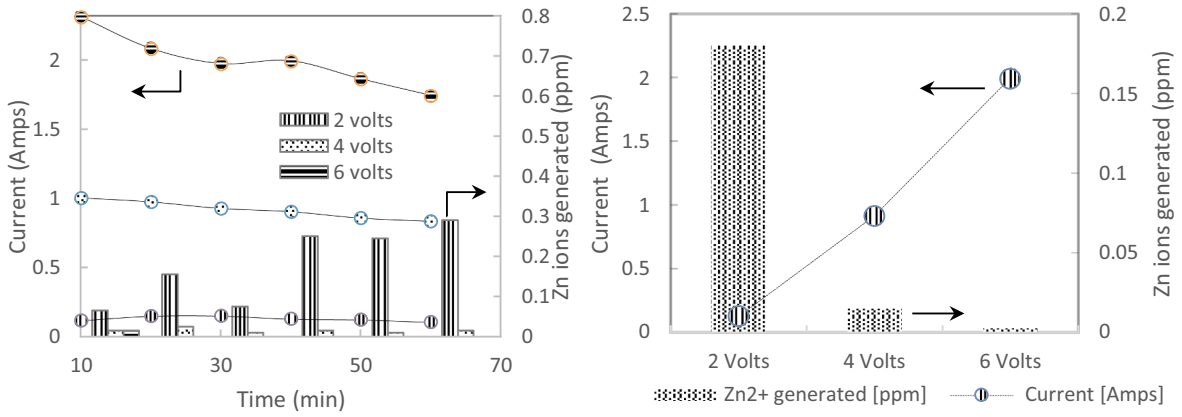

Fig. 4. (Left): Zn^{2+} generation at different voltages and current densities; (Right): average Zn^{2+} generated for each experimental run.

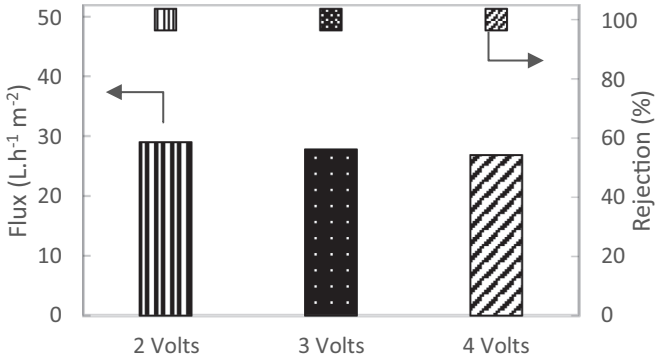

Fig. 5. Effects of Zn^{2+} ions generation voltage on permeate flux and salt rejection.

The flux at a concentration of 2 ppm and 4 ppm was 17.6 and 26.4 $L{\cdot}m^{-2}{\cdot}h^{-1}$, respectively. The difference in flux was due to the $ZnSO_4$ hydrolyzing to sulfate ions as it dissolved in water; which further precipitated calcium; magnesium and other insoluble ions in sulfate salts [17]. In Fig. 6 (right), flux and rejection are demonstrated during Zn^{2+} ion generation. The highest flux of 29.01 $L{\cdot}m^{-2}{\cdot}h^{-1}$ was obtained at 0.2 ppm concentration of Zn^{2+} ions generated using 2 V. The salt rejection of 99% was not influenced by the concentration of $ZnSO_4$ or Zn^{2+} ions generated, thus, showing membrane stability.

3.2.3. Effects of anti-scalant concentration on membrane performance

A gradual decrease in permeate flux was observed during the operational period of all experimental runs, as can be seen in Fig. 7 (left), where two different feed solution concentration of Zn^{2+} ions 0.075 ppm and 0.120 ppm; no anti-scalant; commercial anti-scalant (Vitec 3000), were used. This decline in flux was due to the deposition of particulates followed by the build-up of scale formation on the membrane surface.

The molecular deposition of these dissolved particles and ions at the membrane surface create a locally concentrated layer. Due to the relatively high local concentration, this accumulation tends to reduce the permeate flux through the membrane and hence resulting in a more significant flux decline [18]. However, the flux decline could also be due to an increase in ionic concentration and osmotic pressure during the RO process. The flux decline of the membrane with a dosage of Zn^{2+} ions was lower compared to the operation of the membrane without antiscalant. This showed that Zn^{2+} ions had the ability to suppress scaling through physico-chemical interactions with precipitating species [10]. Trace amounts of Zn^{2+} ions can substantially inhibit the nucleation rate of calcium carbonate crystallization by inducing increases in nucleation times. Thus, the crystal structures of the calcium carbonate formed, changed to aragonite instead of calcite. [19]. The flux decline of the membrane with commercial anti-scalant was reduced to just 5%. The initial flux decreased until it reached the point where it stabilized (after 2 h). This was because the anti-scalant was added at this point. The anti-scalant enhanced the flux rate immediately, and then, the flux rate remained at steady state for the remainder of the experimental time. Limited flux decline was noted after adding the anti-scalant. This is explained by retardation or prevention of the onset of surface crystallization or extremely slow growth of salt crystals on the membrane surface caused by the anti-scalants [12,20].

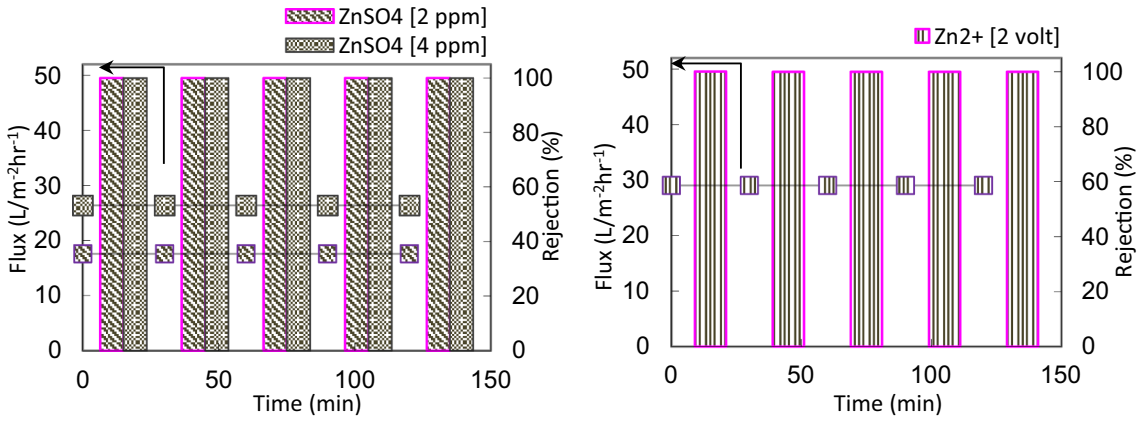

Fig. 6. The comparison of flux decline and a salt rejection of membranes using online Zn^{2+} ions and $ZnSO_4$ as anti-scalant (bench scale).

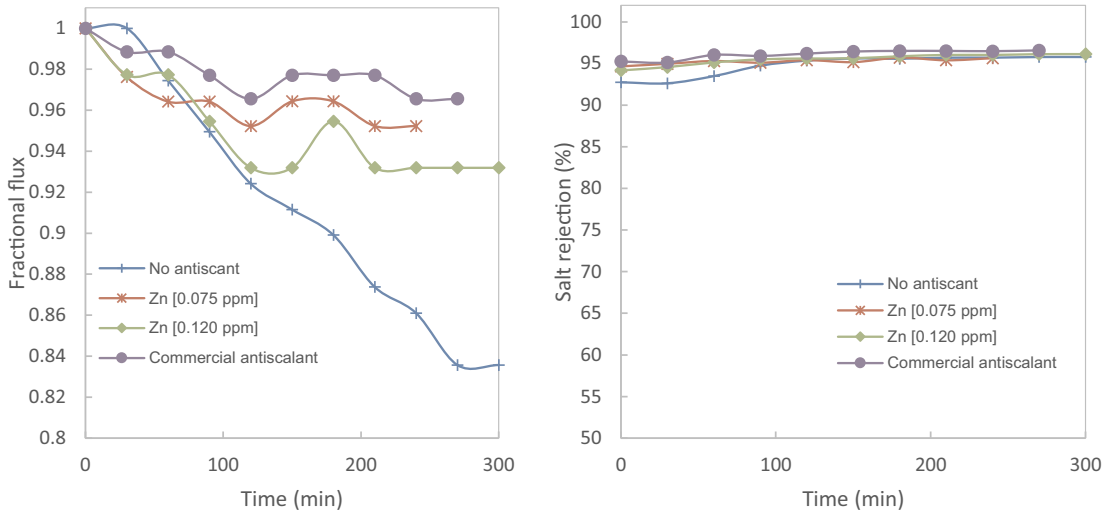

Fig. 7. Flux and salt rejection of scaled RO membrane over time.

3.2.4. Evaluation of anti-scalant on the pilot plant

The pilot plant was operational for close to 5 months (3600 h) (Fig. 8). During this period, the performance of the membranes was closely monitored. The pilot plant consisted of three similar membranes, each subjected to different operating conditions, namely, a membrane treated with commercial anti-scalant, a membrane treated with a concentration of zinc ions not exceeding 20 μg/L (0.02 ppm) and an untreated membrane.

The permeate flux of the membrane treated with commercial anti scalant had the highest value of 32.78 $L{\cdot}m^{-2}{\cdot}h^{-1}$ after 5 months. The membrane treated with zinc ions closely followed this value with a flux of 30.8 $L{\cdot}m^{-2}{\cdot}h^{-1}$. These two membranes performed very well under the conditions and showed no signs of rapid scaling or a sharp decline in the permeate flux. However, the flux for all the membranes lowered significantly, after 30 days, due to raw feed water shortage, which resulted to a reduced inlet feed flow rate to the plant for the rest of the experimental period. The untreated membrane performed the worst of the three membranes with a flux value of 25.56 $L{\cdot}m^{-2}{\cdot}h^{-1}$. When the trend of this membrane was studied it was seen that the permeate flux showed a sharp decline suggesting that the membrane surface is rapidly scaling leading to a loss of permeate quality and permeate flux.

Table 3
The cost estimate of the two anti-scalant methods.

	Anti-scalant	
	Vitec 3000	Zinc ions
Cost per L of feed treated (R)	0.4	–
5 months energy consumption (kWh)	–	14.29
Amount of water treated (kL)	5834.07	5834.07
5 months cost (R)	2333.63	16.89

3.2.5. Scale control cost analysis of the two anti-scalant methods

Comparing scale control cost between the two anti-scalant methodologies were investigated. Table 3 shows the cost estimation of the two anti-scalant over the five-month operational period. The cost of Vitec 3000 as reported by Goldie et al. [15] is R 0.40/kL of feed water treated. For the 5 months period (3600 h) 5834.07 kL were treated. When estimating the cost involved with the membrane treated with zinc ions, the electricity cost of the zinc ion generated was considered. The average current and potential difference over this period were

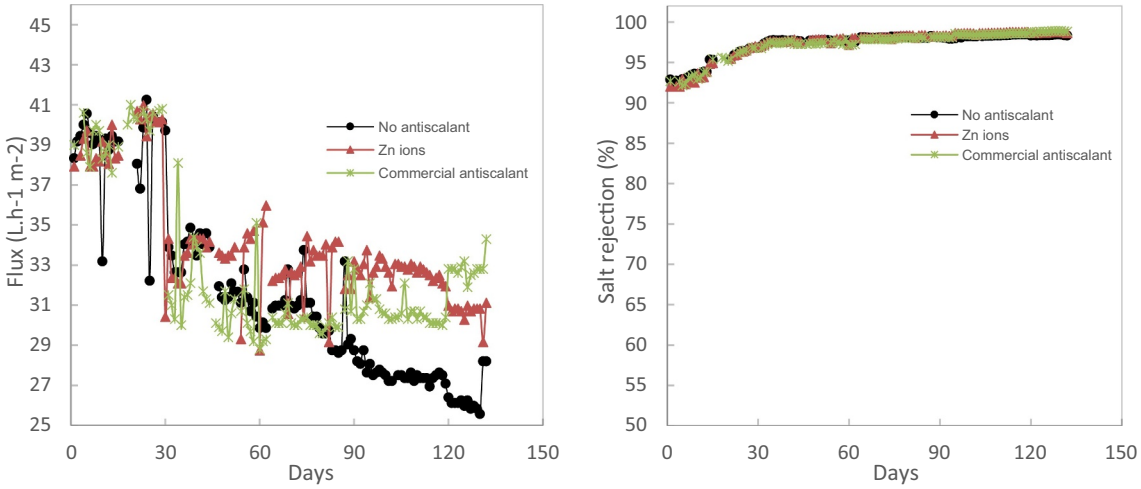

Fig. 8. Pilot plant rejection results of the last four months of operation (Left: permeate flux [$L{\cdot}m^{-2}{\cdot}h^{-1}$], Right: salt rejection [%]).

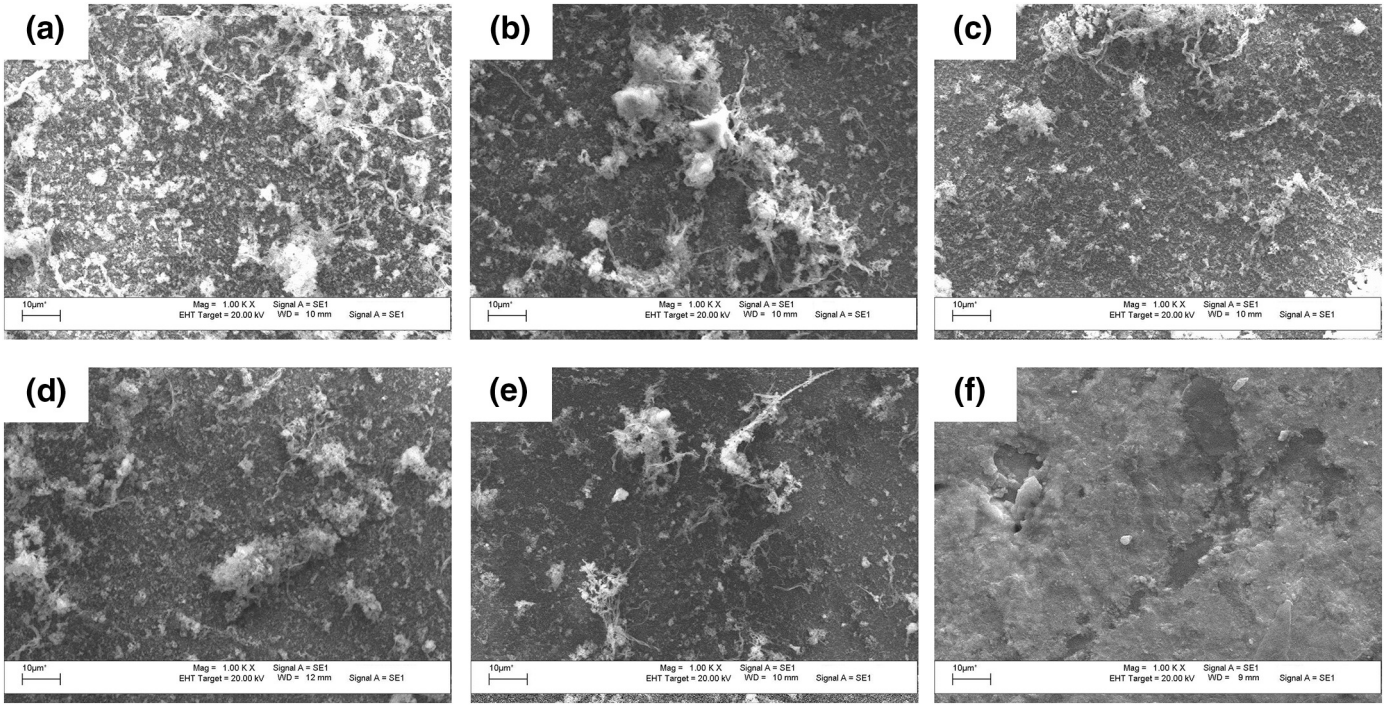

Fig. 9. SEM images of scaled membranes, (a) & (d) untreated; (b) & (e) Zn^{2+} ions; (c) & (f) commercial antiscalant. Bottom: A membrane support layer; Top: membrane polyamide selective layer.

0.557 A and 7.14 V, respectively. The power calculated for the Zn ions generation (dosing) was 14.29 kWh. With an electricity rate of R1.1820/kWh [21], the cost of R16.89 was estimated.

3.2.6. Scaling analysis using scanning electro-magnetic (SEM)

SEM analysis was conducted on the shell and core sides of three thin film composite (TFC) polyamide (PA) Reverse Osmosis (RO) membranes to evaluate the scaling of RO membranes in the presence of the two different anti-scalant. Fig. 9 shows the presence of deposits indicating that scaling occurred. This can be explained by the different mechanisms that include ion pairing, as well as the formation of aggregates and crystals [6]. With the addition of anti-scalant, different agglomeration structures were observed at various surface positions on the membranes. This could be attributed to the gathering of salts [22]. However, scale deposits tend to cover the entire region of the membrane used with no anti-scalant, especially on the core side of the membrane. SEM images of the surface of the membrane treated with commercial anti-scalant showed that the deposits were distributed evenly on the core side than on the shell side. This indicated that the membrane surface at the shell side had fewer deposits. Furthermore, the remaining deposit sizes were smaller than the ones on the untreated membrane. The minimal presence and smaller deposits sizes of grown crystals suggested that the mechanism of scale control by anti-scalant was mainly by the inhibition of crystal nuclei. Thus Zn^{2+} ion solution performed well as an antiscalant in removing the scaling from the surface as a good inhibitor [23].

SEM images from the surface of the membrane treated with Zn^{2+} ions showed that the deposits were more prevalent than the deposits in the case of the membrane treated with the commercial anti-scalant. This means the Zn^{2+} ions eliminated less scaling crystals than the commercial anti-scalant.

3.2.7. Scaling analysis using optical microscopy (OM)

Fig. 10 shows optical microscopy images of scale samples (a) to (d), taken at the feed side of the membranes. Though qualitative in nature they do show scaling took place. The used membranes images showed a dark (brown/black) layer on the surface. These dark spots became more apparent and pronounced on the untreated membrane sample, indicating that scaling was more severe.

4. Conclusions

The main findings of this study were as follows:

- The Zn^{2+} ions generated in the electrolytic cell were at a maximum concentration at a potential difference of 2 V.
- The bench-scale RO cell results confirmed the observations achieved with the SEM images. The flux and rejection of a membrane sample

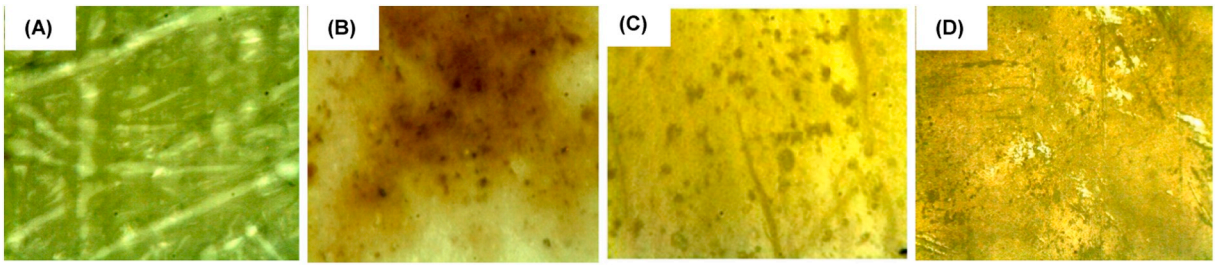

Fig. 10. Comparison of scale formation deposit of (A) virgin membrane, (B) untreated membrane, (C) zinc ions treated membrane and (D) Vitec 3000 treated membrane.

treated with the commercial anti-scalant were higher than membrane samples treated with Zn^{2+} ions and untreated membrane sample, although the Zn^{2+} improved anti-scaling as well.
- Scaling of the membrane in the pilot plant with raw brackish water was lowest with the commercial anti-scalant, followed by the use of Zn^{2+} ions.
- SEM analysis and OM analysis were able to show the morphological changes on the surface of the membranes, compared to an untreated membrane. It also showed that the commercial anti-scalant was more effective than Zn^{2+} ions, as fewer deposits were observed on the membrane surface. Images of the membrane surface treated with the anti-scalant showed that the deposits were distributed evenly on both the active and support layers sides of the membrane. However, deposits on the active layer side were more pronounced.
- The introduction of zinc ions delayed the crystal growth on the membrane surface and results in stability in permeate flux.

Acknowledgements

The authors thank Dr. Ian Goldie and his team at Ikusasa Water (PTY) LTD, Water Research Commission (WRC) and the Cape Peninsula University of Technology (CPUT). The technical support by Wendell Petersen, Judy Maisha, Adel Shames, and Michael Makwonjwa is acknowledged.

References

[1] A. Boubakri, S. Bouguecha, Diagnostic and membrane autopsy of Djerba Island desalination station, Desalination 220 (1–3) (2008) 403–411.
[2] C. Fritzmann, J. Löwenberg, T. Wintgens, T. Melin, State-of-the-art of reverse osmosis desalination, Desalination 216 (1–3) (2007) 1–76.
[3] H.J. Oh, Y.K. Choung, S. Lee, J.S. C hoi, T.M. Hwang, J.H. Kim, Scale formation in reverse osmosis desalination: model development, Desalination 238 (1–3) (2009) 333–346.
[4] S.A. Ali, I.W. Kazi, F. Rahman, Synthesis and evaluation of phosphate-free anti-scalants to control $CaSO_4{\cdot}2H_2O$ scale formation in reverse osmosis desalination plants, Desalination 357 (2015) 36–44.
[5] J. Benecke, M. Haas, F. Baur, M. Ernst, Investigating the development and reproducibility of heterogeneous gypsum scaling on reverse osmosis membranes using real-time membrane surface imaging, Desalination 428 (2018) 161–171.
[6] B.K. Pramanik, Y. Gao, L. Fan, F.A. Roddick, Z. Liu, Antiscaling effect of polyaspartic acid and its derivative for RO membranes used for saline wastewater and brackish water desalination, Desalination 404 (2017) 224–229.
[7] Y. Qingfeng, Inhibition of $CaCO_3$ scaling in reverse osmosis system by zinc ion, Chin. J. Chem. Eng. 14 (2) (2006) 178–183.
[8] S.P. Chesters, F. del Vigo, E.G. Darton, Theoretical and practical experience of calcium phosphate inhibition in RO waters, IDA World Congress on Desalination and Water Reuse, Maspalomas, Gran Canaria, Spain, 2007, October.
[9] I. Goldie, M. Aziz, A. Abozrida, R. Sanderson, Anti-Scaling Studies on High $CaCO_3$ Waters Spiral-Wrap Membrane Systems. Research Report No. 1593/1/08, Water Research Commission, Pretoria, South Africa, 2008.
[10] D. Hasson, R. Semiat, D. Bramson, M. Busch, B. Limoni-Relis, Suppression of $CaCO_3$ scale deposition by anti-scalants, Desalination 118 (1–3) (1998) 285–296 https://www.dupont.com/content/dam/Dupont2.0/Products/water/literature/609-00364.pdf (Accessed 8 Apr. 2019).
[11] J. Wei, J. Liu, M. Li, L. Yang, B. Zhou, The use of the drainage gradient method for evaluating reverse osmosis membrane anti-scalants, Chin. J. Chem. Eng. 14 (2) (2014) 178–183.
[12] D. Lisitsin, Q. Yang, D. Hasson, R. Semiat, Inhibition of $CaCO_3$ scaling on RO membranes trace amounts of zinc ions, Desalination 183 (2005) (2005) 289–300.
[13] P.P. Coetzee, M. Yacoby, S. Howell, S. Mubenga, Scale reduction and scale modification effects induced by Zn and other metal species in physical water treatment, Water SA 24 (1998) 77–84.
[14] A. Sweity, Y. Oren, Z. Ronen, M. Herzberg, The influence of antiscalants on biofouling of RO membranes in seawater desalination, Water Res. 47 (10) (2013) 3389–3398.
[15] I. Goldie, M. Aziz, W. Petersen, D. Mclachlan, Evaluation of Scaling Prevention in Reverse Osmosis Membranes by Anodic Zinc Addition and Magnetic Fields. Research Report No. KV 239/10, Water Research Commission, Pretoria, South Africa, 2010.
[16] E. Lopez-Sandoval, C. Vazquez-Lopez, B. Zendejas-Leal, G. Ramos, E. San Martin-Martinez, N. Munoz Aguirre, E. Reguera, Calcium carbonate scale inhibition using the “allotropic cell” device, Desalination 217 (2007) 85–92.
[17] R.Y. Ning, J.P. Netwig, Complete elimination of acid injection in reverse osmosis plants, Desalination 143 (1) (2002) 29–34.
[18] R. Sheikholeslami, S. Tan, Effects of water quality on silica fouling of desalination plants, Desalination 126 (1–3) (1999) 267–280.
[19] K. Zeppenfeld, Prevention of $CaCO_3$ scale formation by trace amounts of copper (II) in comparison to zinc (II), Desalination 252 (2010) 60–65.
[20] L.F. Greenlee, F. Testa, D.F. Lawler, B.D. Freeman, P. Moulin, The effect of anti-scalant addition on calcium carbonate precipitation for a simplified synthetic brackish water reverse osmosis concentrate, Water Res. 44 (9) (2010) 2957–2969.
[21] Eskom.co.za, Tarrifs & charges 2018/2019, [online] Available at http://www.eskom.co.za/CustomerCare/TariffsAndCharges/Documents/Tariff%20Book.pdf, (2018) , Accessed date: April 2019.
[22] M.K. Shahid, Y.G. Choi, The comparative study for scale inhibition on the surface of RO membranes in wastewater reclamation: CO_2 purging versus three different antiscalants, J. Membr. Sci. 546 (2018) 61–69.
[23] H.J. Meyer, The influence of impurities on the growth rate of calcite, J. Cryst. Growth 66 (1984) 639–646.